Korea-Australia Rheology Journal
Vol. 21, No. 1, March 2009 pp. 17-25

# Investigation of the numerical analysis for the ultrasonic vibration in the injection molding

**Jaeyeol Lee and Naksoo Kim***
*Department of Mechanical Engineering, Sogang University, 1, Sinsu-dong, Mapo-gu, Seoul 121-742, Korea*
(Received August 25, 2008; final revision received November 4, 2008)

## Abstract

We studied the flow characteristics of the polymer melt in the injection molding process with ultrasonic vibration by using the numerical analysis. To minimize the error between the experimental data and numerical result, we presented a methodology using the design of experiments and the response surface method for reverse engineering. This methodology can be applied to various fields to obtain a valid and accurate numerical analysis. Ultrasonic vibration is generally applied between an extruder and the entrance of a mold for improvement the flow rate in injection molding. In comparison with the general ultrasonic process, the mode shape of the mold must be also considered when the ultrasonic vibration is applied on the mold. The mode shape is defined as the periodic and spatial deformation of the structure owing to the effect of the vibration, and it varies greatly according to vibration conditions such as the forcing frequency. Therefore, we considered new index and found the forcing frequency for obtaining the highest flow rate within the range from 20 to 60 kHz on the basis of the index. Ultimately, we presented the methodology for not only obtaining a valid and accurate numerical analysis, but also for finding the forcing frequency to obtain the highest flow rate in injection molding using ultrasonic vibration.

***Keywords*** : polymer, ultrasonic, vibration, numerical analysis, filling process, injection molding

## 1. Introduction

Recently, thin and light-weight products of polymer consumption have been in the limelight. On the other hand, the viscosity characteristic of the polymer melt during the manufacturing of these products raises problems such as the short shot problem. An ultrasonic process is applied to the filling process of injection molding to solve these problems.

Chen and Li (2006; 2007) studied the ultrasonic process when a polymer melt is injected into a thin cavity. Their study concluded that the low viscosity due to ultrasonic vibration caused a decrease in cavity pressure and an increase in the flow rate. Feng and Isayev (2004) along with Swain and Isayev (2007) carried out an experimental study about the interrelation between the ultrasonic intensity and amplitude. Their studies looked at the variation in cavity pressure and examined mechanical properties such as the stress-strain curve with respect to the amplitude of the ultrasonic vibration.

Ho *et al.* (1993) studied the variation of these mechanical properties due to ultrasonic vibration on the polymer melt mixing. Morii *et al.* (1999) performed a research study that investigated the variation of a mechanical property of FRP (fiber reinforced plastics) as a result of the effect of ultrasonic vibration.

In general, there are two primary factors that have influence on the polymer melt due to ultrasonic vibration: the viscosity and the molecular weight. Kim *et al.* (2002) performed an experimental study about the variation of the viscosity with respect to the forcing frequency of the ultrasonic vibration, the applied time of the ultrasonic vibration and mixing temperature in the extruder. Madras *et al.* (2000) carried out an experiment about the variation of the molecular weight due to ultrasonic vibration. Kanwal *et al.* (2000) studied the decrease of the molecular weight and the variation in the mechanical properties with respect to the ultrasonic time. With respect to the ultrasonic intensity and time, Li *et al.* (2005) carried out a research study that investigated the variations of the viscosity and the molecular weight of two polymer melts: polystyrene and ethylene-propylene diene monomer.

Price *et al.* (2002) additionally studied the variation of the molecular weight as well as the melting point due to ultrasonic vibration. Sahnoune and Piche (1998) performed a research study that investigated the variation of a thermal property such as the thermal expansivity of the polymer melt. Shim *et al.* (2002) carried out an experimental study on the number and diameter of bubbles in the polymer melt with respect to the ultrasonic intensity and pressure in the polymer melt.

On the other hand, there are also many studies about the

*Corresponding author: nskim@sogang.ac.kr

numerical analysis used to predict the behavior of the polymer melt in injection molding. Buchmann *et al.* (1997) experimentally investigated viscosity models of the polymer melt. On the basis of these viscosity models, the numerical analysis was utilized to predict the flow characteristic of the polymer melt with respect to the injection conditions. Kim *et al.* (2006a; 2006b) and Ye *et al.* (2005) numerically analyzed the behavior of the polymer melt in the extruder using FVM (finite volume method). Mousavi *et al.* (2007) performed a numerical analysis to predict the decrease of the extruder force with respect to an increase in the ultrasonic intensity using FEM (finite element method).

In a preceding study, Lee and Kim (2008) numerically analyzed the flow rate of the polymer melt with respect to the mode shapes of a mold and investigated the characteristics of the mode shape to find a more efficient mode shape for high flow rates. Lee *et al.* (2008) also studied injection conditions and vibration conditions for a higher filling efficiency.

In this study, we compared our numerical results with the experimental results of Chen and Li (2006) to verify the validity of the numerical analysis. Using this numerical analysis, we modeled the injection of the polymer melt into a thin cavity and investigated the flow rate of the polymer melt with respect to the forcing frequency of the ultrasonic vibration. Ultimately, we introduced a methodology for finding the forcing frequency at the highest flow rate.

## 2. Theory

### 2.1. Ultrasonic vibration

A piezoelectric transducer generates an ultrasonic vibration from an applied AC (alternating current), and an ultrasonic horn is a device used to amplify this vibration. As a result, the polymer melt in the cavity is filled due to the effect of this ultrasonic vibration. When this ultrasonic vibration propagates, the vibrational energy in a unit area vertical to the direction of propagation is known as the intensity (Li *et al.*, 2005), and is as follows:

$$I = 2\pi^2 \rho c f^2 x^2 = A f^2 x^2, \tag{1}$$

where $\rho$ is the density of the material, $c$ is the propagation velocity of the ultrasonic vibration, $f$ is the forcing frequency of the ultrasonic vibration and $x$ is the amplitude of the ultrasonic vibration. The forcing frequency of the ultrasonic vibration is generally 20 kHz or more, which causes the intensity to be very high.

### 2.2. Governing equation

In general, the polymer melt is a non-Newtonian fluid. Its flow characteristics are incompressible and laminar. To express these flow characteristics in the Cartesian coordinate system, the continuity and momentum equations (Kim *et al.*, 2006a) are given as follows:

$$\frac{\partial \rho}{\partial t} + \frac{\partial}{\partial x_j}(\rho u_j) = s_m, \tag{2}$$

$$\frac{\partial (\rho u_i)}{\partial t} + \frac{\partial}{\partial x_j}(\rho u_j u_i - \tau_{ij}) = -\frac{\partial p}{\partial x_i} + s_i, \tag{3}$$

$$\frac{\partial (\rho h)}{\partial t} + \frac{\partial}{\partial x_j}(\rho h u_j + F_{h,j}) = \frac{\partial p}{\partial t} + u_j \frac{\partial p}{\partial x_j} + \tau_{ij}\frac{\partial u_i}{\partial x_j} + s_h. \tag{4}$$

These equations are calculated using the PISO (pressure implicit with splitting of operators) algorithm in FVM. The flux term is solved by the upwind scheme. The shear stress is expressed by the following constitutive law.

$$\tau_{ij} = 2\mu s_{ij} - \frac{2}{3}\mu \frac{\partial u_k}{\partial x_k}\delta_{ij}, \tag{5}$$

where $s_{ij} = \frac{1}{2}\left(\frac{\partial u_i}{\partial x_j} + \frac{\partial u_j}{\partial x_i}\right)$.

### 2.3. Carreau-WLF model

The Carreau-WLF (Williams-Landel-Ferry) model is considered as a viscosity model of the polymer melt. This model is the modified Carreau-Yasuda model, which includes temperature dependence by using a WLF relation and is written as follows:

$$\mu = \frac{k_1 a_T}{[1 + k_2 \dot{\gamma} a_T]^{k_3}}, \tag{6}$$

where $\ln a_T = \frac{8.86(k_4 - k_5)}{101.6 + k_4 - k_5} - \frac{8.86(T - k_5)}{101.6 + T - k_5}$

and $\dot{\gamma} = \sqrt{\frac{1}{2}(s_{ij}s_{ij} - s_{ii}s_{jj})}$.

As shown in equation (6), the Carreau-WLF model (Buchmann *et al.*, 1997) includes both the deformation rate ($\dot{\gamma}$) and shift ($a_T$) as a function of temperature. $k_1$, $k_2$, $k_3$, $k_4$ and $k_5$ are material-dependent constants. This viscosity model is transformed to a user subroutine in the FVM calculation.

### 2.4. Design of experiments using the orthogonal array table

Design of experiments is defined as a plan of experiments that includes the method of setting up an experiment about a problem, method of data collection and method of obtaining the maximum amount of information in the minimum number of experiments based on statistical data analysis (Lim *et al.*, 1999). In other words, using design of experiments requires the selection of parameters about a problem, selection of an experimental method, decision on the experiment order and selection of the optimum analysis method for the data obtained from the experiment.

There are many parameters to be considered in general.

The orthogonal array table not only considers all parameters, but also excludes information about the interaction between parameters. As a result, the number of a numerical analysis or experiments can be minimized. We can also easily analyze the effect of parameters from the results.

### 2.5. Response surface method

RSM (response surface method) is a chain of processes that assumes a relation between the parameters and the response function as a mathematical equation, assumes a coefficient of the equation with the least squares method from results, and then makes a useful response surface model (Youn and Choi, 2004). In this study, a second response surface model is used as follows:

$$y = \beta_0 + \sum_{i=1}^{n_d} \beta_i x_i + \sum_{i=1}^{n_d} \sum_{j \geq i}^{n_d} \beta_{ij} x_i x_j , \quad (7)$$

where $x_i$ is the parameter, $n_d$ is the number of the parameter and $\beta_i$ is coefficient assumed by the least squares method.

Equation (8) is the calculation method of the coefficient of the response surface model.

$$\beta = (\mathbf{X}^T\mathbf{X})^{-1}\mathbf{X}^T\mathbf{Y} , \quad (8)$$

where **X** is a parameter matrix composed of experimental points and **Y** is a response vector.

### 2.6. Forced vibration

A forced vibration occurs when a structure is influenced by a periodic external force or displacement. The forced vibration (Orhan, 2007) can be expressed by the following equation.

$$\mathbf{M}\ddot{\mathbf{x}} + \mathbf{C}\dot{\mathbf{x}} + \mathbf{K}\mathbf{x} = \mathbf{F}_o \sin\omega t , \quad (9)$$

where **M** is a mass of the vibrated structure, **C** is a damping constant, **K** is a spring constant, **x** is a displacement, $\omega$ is a forcing frequency and t is a time period. If the external force ($\mathbf{F}_o$) is zero, this equation reduces down to a free vibration.

## 3.Verification of the numerical analysis

### 3.1. Geometry and material properties

Chen and Li (2006) experimentally investigated the flow rate of PS (polystyrene). Fig. 1(a) shows the geometry of the extruder system that is used for their experiment. On the basis of this extruder system, we modeled an analysis domain for analyzing the filling process in the cavity as shown in Fig. 1(b). They concluded that the flow rate of PS increased with an increase in the intensity at the same cavity pressure as shown in Fig. 2.

To verify the validity of our numerical analysis, we compared the numerical results with the experimental data of Chen and Li (2006). FVM was used in this numerical analysis for the behavior of the polymer melt in the filling process. We used the commercial code STAR-CD for this FVM calculation. A vibration phenomenon, which occurs on the surfaces of a cavity or mold due to ultrasonic vibration, is also applied to the velocity and wall boundary conditions using the moving grid method. The rest of the injection and boundary conditions are applied with reference to the experiment of Chen and Li (2006).

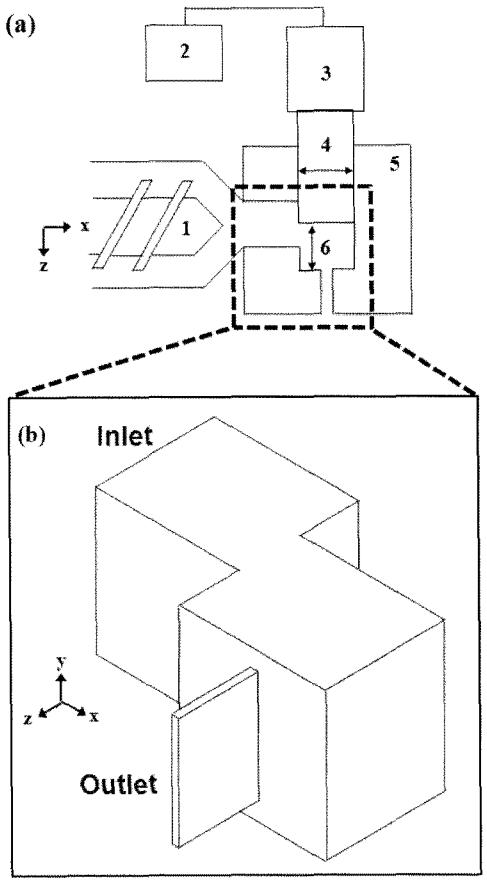


**Fig. 1.** Geometry of the extruder system; (a) geometry in the experimental study of Chen and Li (2006): 1, extruder; 2, ultrasonic generator; 3, piezoelectric transducer; 4, ultrasonic horn with diameter $\phi$=10 mm; 5, cavity; 6, the gap between the horn tip and entry to the cavity is 10 mm, (b) geometry of the analysis domain.

### 3.2. Applications of the orthogonal array and RSM

It is generally difficult to measure the viscosity of the polymer melt flowing inside of the mold to determine the viscosity characteristic. In addition to this inherent difficulty, there is also the possibility of measurement error. Therefore, it is necessary to investigate these material properties in order to make sure of the accuracy and validity of the results, especially in the numerical analysis. For this reason, we considered the parameters $k_1$, $k_2$ and $k_3$ in equation (6) to be constant values, while both $k_4$ and $k_5$ are not considered in the analysis since the effect of temper-

**Table 1.** Table of orthogonal arrays

| No. | $k_1$ | $k_2$ | $k_3$ | Φ |
|---|---|---|---|---|
| 1 | 5000 | 0.064 | 0.81 | 34.38 |
| 2 | 5000 | 0.065 | 0.83 | 4.08 |
| 3 | 5000 | 0.066 | 0.85 | 43.58 |
| 4 | 5100 | 0.064 | 0.85 | 13.42 |
| 5 | 5100 | 0.065 | 0.81 | 41.50 |
| 6 | 5100 | 0.066 | 0.83 | 6.11 |
| 7 | 5200 | 0.064 | 0.83 | 29.80 |
| 8 | 5200 | 0.065 | 0.85 | 9.67 |
| 9 | 5200 | 0.066 | 0.81 | 46.25 |

ature is minor. Each parameter is classified to 3 levels and Table 1 shows the values of the parameters according to their level and the composition of the table of the orthogonal array $L_9(3^4)$.

In this study, the object function (Φ) is the total error rate between the experimental data (y) and the numerical result (y') as shown in equation (10).

$$\Phi = \sum \left| \frac{y - y'}{y} \times 100 \right|. \quad (10)$$

As a result of the numerical analysis, the object function is shown in equation (11) as a function of the constant values using the response surface method.

$$\Phi = 30683.046 + 8351.863k_1 - 5164.352k_2 - 8418.794k_3 + 198.074k_1^2 + 260.141k_2^2 + 525.548k_3^2 - 577.235k_1k_2 + 563.611k_2k_3 - 790.084k_1k_3. \quad (11)$$

The parameters of the minimum object function, along with the minimum total error rate between the experimental and the numerical results are shown as follows:

$$k_1 = 5000 \quad k_2 = 0.06503 \quad k_3 = 0.82811,$$

where the constraints of the parameters $k_1$, $k_2$ and $k_3$ are set to be from 5000 to 5200, 0.064 to 0.066 and 0.81 to 0.85, respectively, but the initial values of the parameters are 5000, 0.066 and 0.81, respectively.

### 3.3. Investigation of the amplitude due to the ultrasonic vibration

The amplitude of the ultrasonic vibration is the most important parameter that has influence on the flow characteristic of the polymer melt in the ultrasonic process: therefore, we used RSM for the investigation of the amplitude. The initial values of the amplitude are 0.05, 0.15 and 0.25 μm. As shown in equation (10), the object function is a total error rate when the intensities are 50, 100, 150 and 200 W. As a result, the object function is shown in equation (12) as a function of the amplitude using the response surface method.

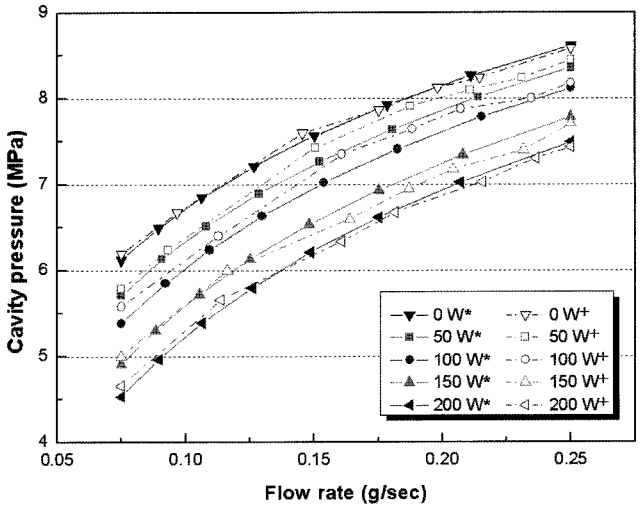


**Fig. 2.** Comparison of the results [* : computational results, + : experimental results of Chen and Li (2006)].

$$\Phi = 4691.126 - 53978.858x + 213904.670x^2, \quad (12)$$

where $x$ is the amplitude (μm) at 50 W and $x$ as the amplitude at 50 W is 0.130 μm. Additionally, the amplitudes of 100, 150 and 200 W are calculated on the basis of equation (1) as a function between the intensity and the amplitude of the ultrasonic vibration.

### 3.4. Results and discussions

We compared the numerical results with the experimental data to verify the validity of our numerical analysis as shown in Fig. 2. The flow rate of PS increases with an increases in the cavity pressure and intensity.

In particular, the two results between the numerical analysis and the experimental study have a slight difference without the ultrasonic vibration. Over-all, there is little difference between the numerical and experimental results despite several error factors including: the variation of the material properties of the polymer melt due to pressure, the generation of cavitations owing to a phase change of the polymer melt and the effect of measurement errors.

In conclusion, the numerical analysis in this study is a valid method for analyzing the filling process of injection molding by use of ultrasonic vibration. We also indicated the method of obtaining the accuracy of the numerical analysis as the methodology of using both the design of experiments and response surface method for reverse engineering. This method can be used for not only the numerical analysis of injection molding but also for various other fields of study.

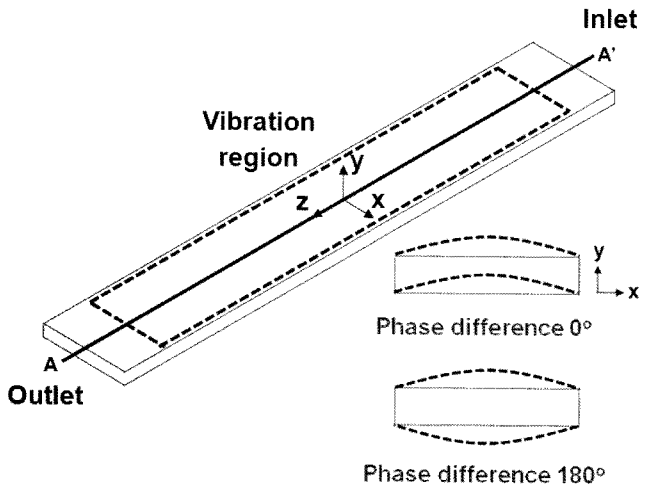


**Fig. 3.** Analysis domain of the cavity.

## 4. Flow characteristics with the ultrasonic vibration

### 4.1. Analysis domain

We used the same numerical analysis to study the flow characteristics of the polymer melt when a periodic deformation on the cavity surfaces occurs due to the effect of ultrasonic vibration. Fig. 3 shows the analysis domain and illustrates the deformation on both the upper (positive $y$-directional) and lower (negative $y$-directional) cavity surface with respect to the phase difference.

This domain is the cavity ($200\times20\times2$ mm$^3$). The polymer melt at the inlet is injected into the cavity and is ejected out of the cavity through the outlet after it passes through the vibration region. The vibration region, which is assumed to simplify the analysis, is composed of both the upper and lower cavity surfaces. If the boundary conditions are not separately mentioned in this study, then the injection conditions are the following constant values: inlet pressure of 60 MPa, inlet temperature of 473.15 K, mold temperature of 323.15 K, outlet pressure of 0 MPa and outlet temperature of 323.15 K.

We investigated the variation of the flow rate as the flow characteristic due to the phase difference. The phase difference is the difference between the motion directions of the upper and lower cavity surfaces. For example, in the case of 180° phase difference, the upper cavity surface moves in the positive $y$-direction, while the lower cavity surface moves in the negative $y$-direction. In other words, it is with the 180° phase difference that one motion direction is opposite of the other.

One of our prior studies already concluded that the effect of the $y$-directional motion is higher than that of the $x$-directional motion for the improvement of flow rate from the standpoint of flow physics. Therefore, this study only considered the y-directional motion on the cavity surfaces.

**Table 2.** Constant values of polymer materials

| | HDPE | LDPE | PP |
|---|---|---|---|
| $\Delta H/R$ [K] | 3623.6 | 7460.7 | 7537.5 |
| $\lambda$ [sec] | 10.32 | 3.28 | 0.13 |
| $\mu_o$ [Pa-sec] | 36775 | 5645 | 2410 |
| $n$ | 0.53 | 0.61 | 0.43 |

**Table 3.** MFI with respect to the phase difference

| Phase difference | MFI of HDPE | MFI of LDPE | MFI of PP |
|---|---|---|---|
| No vibration | 0.103 | 0.010 | 0.019 |
| 0 | 0.105 | 0.011 | 0.029 |
| 180 | 1.323 | 0.388 | 1.180 |

### 4.2. Viscosity model

This study considered three polymer melts: HDPE (high density polyethylene), LDPE (low density polyethylene) and PP (polypropylene). The viscosity model for the numerical analysis is considered to be the Carreau model as expressed in equation (13).

$$\mu=\mu_o a_T[1+(\lambda a_T\dot{\gamma})^2]^{(n-1)/2}, \tag{13}$$

where $a_T=\exp\left[\frac{\Delta H}{R}\left(\frac{1}{T}-\frac{1}{T_o}\right)\right]$

and $\dot{\gamma}=\sqrt{\frac{1}{2}(s_{ij}s_{ij}-s_{ii}s_{jj})}$,

where $a_T$ is the shift, $\dot{\gamma}$ is the deformation rate, $\lambda$ is the time constant, $\mu_o$ is the zero shear rate viscosity and $n$ is the power-law index. Each value is shown in Table 2. We referred to the study of Collier *et al.* (2003) for these values.

### 4.3. Results

This study used MFI (melt flow index, g/sec) as an index for the estimation of the flow rate of the polymer melt. MFI is defined as the total mass flow passing the flow cross section per unit time. Table 3 shows the MFI of each polymer melt with respect to the phase difference.

The MFI of HDPE is the highest, whereas the MFI of LDPE is the lowest regardless of the phase difference. On the other hand, the MFI with a 180° phase difference is the highest, whereas MFI without the ultrasonic vibration is the lowest within each polymer material.

From the standpoint of flow physics, the primary characteristic of the phase difference is the periodic change of the flow cross section; the magnitude of the flow cross sec-

tion with a 180° phase difference changes periodically, whereas that of the flow cross section with a 0° phase difference does not change. In other words, the flow rate is only affected by the vibrational energy that is transmitted from the cavity surface to the polymer melt in the case of the 0° phase difference, but the flow rate is not only affected by this but also by the pumping effect in the case of the 180° phase difference. The pumping effect is the phenomenon of improving the flow rate and is caused by the periodic change of the flow cross section, like in a pump. As a result, the flow rate for the 180° phase difference is higher than that for 0° the phase difference.

## 5. Investigation of MFI with respect to the forcing frequency

### 5.1. Intensity factor and pumping factor

On the basis of the above results, we present two new indexes for the prediction of the flow rate in the filling process with ultrasonic vibration as follows:

$$IF = [\int(f^2 y^2)dx]/L$$
$$PF = [\int ydx]/L, \quad (14)$$

where $f$ is the forcing frequency (kHz) of the ultrasonic vibration, $y$ is the $y$-directional amplitude (μm) of the upper cavity surface due to the vibration, $L$ is the $z$-directional length (200 mm) of the cavity. IF (intensity factor) is the vibrational energy per unit length that is transmitted from the cavity surface to the polymer melt due to ultrasonic vibration. On the other hand, PF (pumping factor) is the maximum change of the flow cross section in the cavity per unit length owing to ultrasonic vibration.

### 5.2. Forced vibration analysis of the mold

We modeled a mold to investigate the periodic deformation of the cavity due to ultrasonic vibration as shown in Fig. 4.

**Table 4.** Material properites of S45C

| | |
|---|---|
| Young's modulus (GPa) | 206 |
| Shear modulus (GPa) | 79 |
| Density (kg/m$^3$) | 7600 |
| Poisson's ratio | 0.298 |

The mold ($220 \times 60 \times 30$ mm$^3$) is vibrated by an external force (0.1N) in the middle ($20 \times 20$ mm$^2$) of the upper mold, while the contact condition is applied between the upper and lower mold. The constraint condition is also applied at the bottom of the mold and at the guide pins ($\phi$=8 mm).

Table 4 shows the material properties of the mold used for the forced vibration analysis. We referred to the study of Chen and Kim (2003) for these values and used the commercial code ANSYS for the FEM calculation of this analysis.

A mode shape is a specific pattern of the deformation of the vibrated structure at a specific forcing frequency. The mode shapes can generally be classified as two flexural modes and a torsional mode with respect to the primary direction of the deformation. Therefore, the frequency response is used for investigation of this deformation with respect to the forcing frequency.

Fig. 5 shows the frequency response that results in the middle of the upper cavity surface with respect to the forcing frequency (20 to 60 kHz). The peak point does not exist below 30 kHz, which means that there is no response of the mold below a forcing frequency of 30 kHz. As a result, it is hard to obtain a high flow rate because of the unchanged amplitude in this range of the forcing frequency. On the contrary, there are many peak points

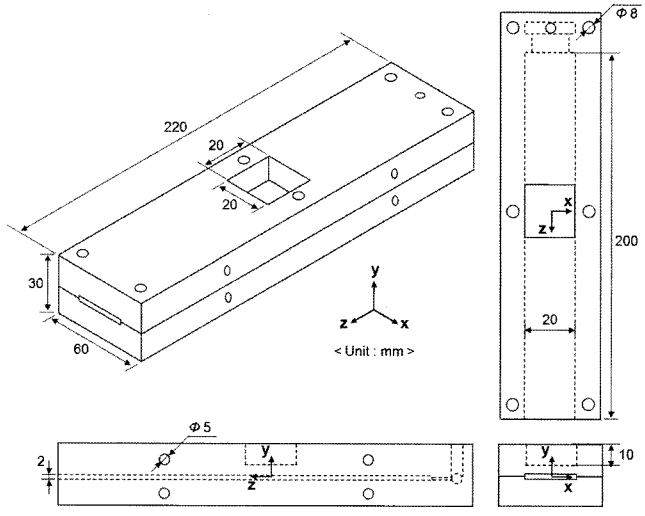


**Fig. 4.** Dimensions of the mold.

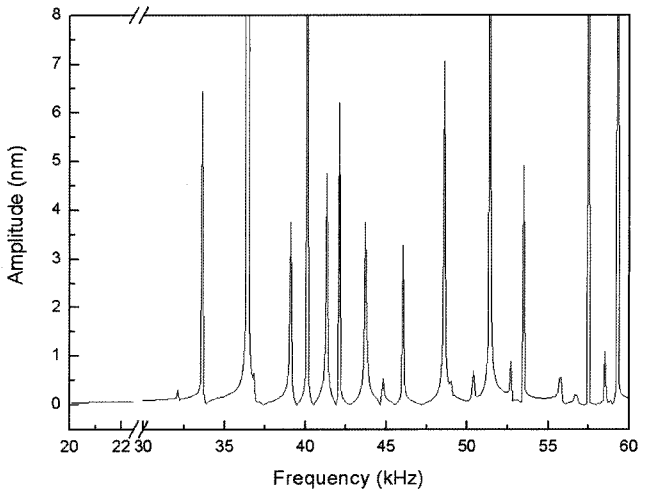


**Fig. 5.** Frequency response.

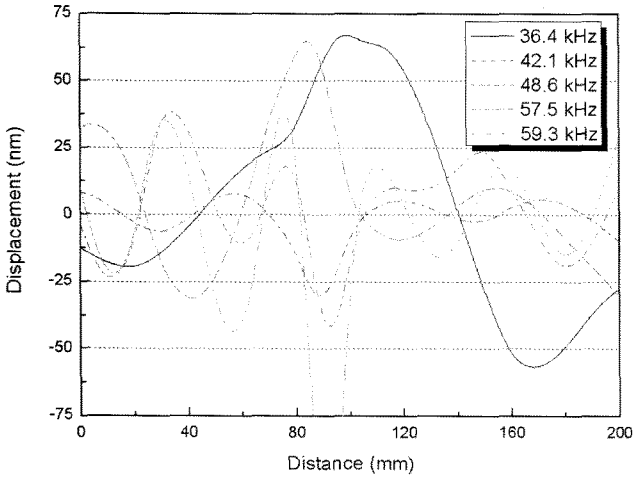


**Fig. 6.** Deformation of the upper cavity surface.

throughout the rest of the forcing frequency range, which indicates that a high flow rate can be obtained if the mold is vibrated at the forcing frequency of the peak point.

To investigate the forcing frequency for this high flow rate, we calculated IF and PF as defined in equation (13) on the basis of the frequency response in A-A' of Fig. 3. As a result, we selected total five forcing frequencies: 59.3, 36.4, 42.1, 57.5 and 48.6 kHz. We predicted that the flow rate at 59.3 kHz is the highest among these frequencies, whereas the flow rate at 48.6 kHz is the lowest.

Fig. 6 shows the deformation of the upper cavity surface with respect to the forcing frequency. The distance in this case is the distance from the inlet of the cavity to the outlet. For example, the distance of 200 mm is the outlet of the cavity. The wavelength, which is defined as the distance between repeating units of a propagating wave, decreases as the forcing frequency increases, similar to the general pattern of deformation due to vibration. In the case of the same forcing frequency, the deformation at a distance of 90 to 110 mm is the largest because this region is closest to the external force.

To confirm the flow rate at each forcing frequency, Table 5 shows the MFI of the three polymer melts with respect to the forcing frequency. We predicted the order of the flow rate according to the forcing frequency on the basis of the multiplication of IF with PF. This value is the highest at 59.3 kHz as shown in Table 5. Therefore, we predicted that the flow rate at 59.3 kHz is the highest regardless of the type of polymer material. Over-all, these results are similar to the prediction given by the calculations of IF and PF. We concluded that the order of the flow rate is similar to the predicted order as a result of the flow analysis. On the other hand, the order of the flow rate between 57.5 and 48.6 kHz is different from the predicted order due to the complicated and local flow characteristics of the polymer melt that is caused by the deformation of the cavity as shown in Fig. 6.

**Table 5.** MFI with respect to the forcing frequency

| Frequency (kHz) | IF×PF | MFI of HDPE | MFI of LDPE | MFI of PP |
|---|---|---|---|---|
| 59.3 | 0.111 | 0.558 | 0.112 | 0.381 |
| 36.4 | 0.066 | 0.492 | 0.095 | 0.309 |
| 42.1 | 0.022 | 0.400 | 0.084 | 0.242 |
| 57.5 | 0.020 | 0.248 | 0.049 | 0.125 |
| 48.6 | 0.001 | 0.248 | 0.056 | 0.148 |

In conclusion, we predicted that the flow rate at 59.3 kHz is the highest in the range from 20 to 60 kHz of the forcing frequency on the basis of the multiplication of IF and PF. The result of the flow analysis shows that the flow rate is the highest at 59.3 kHz.

## 6. Conclusions

We studied the flow characteristics of the polymer melt in the injection molding process with ultrasonic vibration by using the numerical analysis. We modeled the same extruder system as the experiment by Chen and Li (2006) and compared the numerical results with the experimental data. Also, we present two new indexes for the prediction of the flow rate according to the forcing frequency.

In the previous study, we applied the constant value of the viscosity model for PS on the basis of the reference. As a result, there are some differences between the experimental data and the numerical result in the previous study. On the other hand, we used the reverse engineering using both the design of experiments and response surface method to minimize the error between the experimental and numerical result in this study. So, the numerical results in this study are more accurate than those in the previous study.

We ultimately presented the methodology for not only obtaining a valid and accurate numerical analysis, but also for finding the forcing frequency to obtain the highest flow rate in injection molding using ultrasonic vibration. We are to carry out an experiment to verify this study.

From the results, we obtained the following conclusions.

1) To obtain a valid and accurate numerical analysis, we presented the methodology using both the design of experiments and response surface method. As a result, the total error rates between the experimental data and the numerical result are 4% and below.
2) The MFI of HDPE is the highest within each polymer material, whereas the MFI of LDPE is the lowest regardless of the phase difference.
3) The MFI with a 180° phase difference is the highest, whereas MFI without the ultrasonic vibration is the

lowest. In other words, the flow rate for the 180° phase difference is higher than that for 0° the phase difference.

4) As a result of the forced vibration (20 to 60 kHz) of the mold, there is no response of the mold below a forcing frequency of 30 kHz. In other words, it is hard to obtain a high flow rate because of the unchanged amplitude in this range of the forcing frequency.
5) We predicted that the flow rate at 59.3 kHz is the highest in the range from 20 to 60 kHz of the forcing frequency on the basis of the multiplication of IF and PF. The result of the flow analysis shows that the flow rate is the highest at 59.3 kHz.

## Acknowledgments

This work was supported by Korean Research Foundation Grant (KRF-2006-005-J02302).

## Nomenclatures

| | |
|---|---|
| $A$ | : Constant |
| $a_T$ | : Temperature shift factor |
| $\mathbf{C}$ | : Damping constant |
| $c$ | : Propagating velocity of the ultrasonic vibration |
| $F_{h,j}$ | : Diffusional energy flux in the $x_j$-direction |
| $\mathbf{F}_o$ | : External force |
| $f$ | : Frequency of the ultrasonic vibration |
| $h$ | : Enthalpy |
| $I$ | : Vibration intensity |
| $k_i$ | : Constants in Carreau-WLF model |
| $\mathbf{K}$ | : Spring constant |
| $\mathbf{M}$ | : Mass of the vibrated structure |
| $n$ | : Power-law index |
| $n_d$ | : The number of the parameter |
| $p$ | : Pressure |
| $s_m$ | : Mass source term |
| $s_i$ | : Momentum source term |
| $s_h$ | : Energy source term |
| $s_{ij}$ | : Strain rate tenser |
| $t$ | : Time |
| $T$ | : Temperature |
| $T_{ref}$ | : Reference temperature |
| $u_i$ | : Velocity component in the $x_j$-direction |
| $u, v, w$ | : Velocity components in the $x$-, $y$-, $z$-directions, respectively |
| $x$ | : Amplitude of the ultrasonic vibration |
| $x_j$ | : Cartesian coordinate ($j=1, 2, 3$) |
| $\mathbf{x}$ | : Displacement |
| $x_i$ | : Parameters |
| X | : Parameter matrix |
| Y | : Response vector |
| $y$ | : $y$-directional amplitude of the upper cavity surface |

## Greek symbols

| | |
|---|---|
| $\beta$ | : Coefficient of the response surface model |
| $\delta_{ij}$ | : Kronecker delta |
| $\dot{\gamma}$ | : Deformation rate |
| $\lambda$ | : Time constant |
| $\mu$ | : Viscosity |
| $\mu_0$ | : Zero shear viscosity |
| $\rho$ | : Density |
| $\tau_{ij}$ | : Stress tensor components |
| $\omega$ | : Forcing frequency |

## References

Buchmann, M., R. Theriault and T. A. Osswald, 1997, Polymer flow length simulation during injection mold filling, *Polymer Eng. and Sci.* **37**, 667-671.

Chen, X. and K. S. Kim, 2003, Modeling of ratcheting behavior under multiaxial cyclic loading, *Acta Mechanica* **163**, 9-23.

Chen, Y. and H. Li, 2006, Effect of ultrasound on the viscoelasticity and rheology of polystyrene extruded through a slit die, *J. of Appl. Polymer Science* **100**, 2907-2911.

Chen, Y. and H. Li, 2007, Mechanism for effect of ultrasound on polymer melt in extrusion, *J. of Polymer Sci.* **45**, 1226-1233.

Collier, J. R., S. Petrovan and P. Patil, 2003, Temperature shifting of convergent flow measured effective elongational viscosity, *J. of Appl. Polymer Science.* **87**, 1387-1396.

Feng, W. and A. I. Isayev, 2004, In situ compatibilization of PP/EPDM blends during ultrasound aided extrusion, *Polymer* **45**, 1207-1216.

Ho, R. M., A. C. Su and C. H. Wu, 1993, Functionalization of polypropylene via melt mixing, *Polymer* **34**, 3264-3269.

Kanwal, F., J. J. Liggat and R. A. Pethrick, 2000, Ultrasonic degradation of polystyrene solutions, *Polymer Degradation and Stability* **68**, 445-449.

Kim, H. S., J. G Ryu and J. W. Lee, 2002, Evolution of phase morphology and in-situ compatibilization of polymer blends during ultrasound-assisted melt mixing, *Korea-Australia Rheol. J.* **14**, 121-128.

Kim, N. S., H. B. Kim and J. W. Lee, 2006a, Numerical analysis of internal flow and mixing performance in polymer extruder I: single screw element, *Korea-Australia Rheol. J.* **18**, 143-151.

Kim, N. S., H. B. Kim and J. W. Lee, 2006b, Numerical analysis of internal flow and mixing performance in polymer extruder II: twin screw element, *Korea-Australia Rheol. J.* **18**, 153-160.

Lee, J. Y. and N. S. Kim, 2008, Prediction of charging rate in ultrasonic vibration of injection molding, *Journal of Materials Processing Technology* **201**, 710-715.

Lee, J. Y., N. S. Kim and J. W. Lee, 2008, Numerical analysis of injection molding for filling efficiency on ultrasonic process, *Korea-Australia Rheol. J.* **20**, 79-88.

Li, J., S. Guo and X. Li, 2005, Degradation kinetics of polystyrene and EPDM melts under ultrasonic irradiation, *Polymer Degradation and Stability* **89**, 6-14.

Lim, J. M., S. Han, S. Jeon, D. Woo and G J. Park, 1999, Analysis and design considerations of energy absorbing steering

system using orthogonal arrays, *Trans. KSAE* **7**, 144-155.

Madras, G., S. Kumar and S. Chattopadhyay, 2000, Continuous distribution kinetics for ultrasonic degradation of polymers, *Polymer Degradation and Stability* **60**, 73-78.

Morii, T., N. Ikuta and H. Hamada, 1999, Influence of ultrasonic vibration frequency on acceleration of hydrothermal aging of FRP, *J. of Thermoplastic Composite Materials* **12**, 465-476.

Mousavi, S. A. A. A., H. Feizi and R. Madoliat, 2007, Investigations on the effects of ultrasonic vibrations in the extrusion process, *J. of Materials Processing Tech.* **187-188**, 657-661.

Orhan, S., 2007, Analysis of free and forced vibration of a cracked cantilever beam, *NDT&E Inter.* **40**, 443-450.

Price, G. J., E. J. Lenz and C. W. G. Ansell, 2002, The effect of high-intensity ultrasound on the ring-opening polymerization of cyclic lactones, *European Polymer J.* **38**, 1753-1760.

Sahnoune, A. and L. Piche, 1998, Ultrasonic study of anharmonicity in amorphous polymers: temperature, pressure and molecular weight effects, *J. of Non-Crystalline Solids* **235-237**, 664-669.

Shim, S. E., S. Ghose and A. I. Isayev, 2002, Formation of bubbles during ultrasonic treatment of cured poly(dimethyl siloxane), *Polymer* **43**, 5535-5543.

Swain, S. K. and A. I. Isayev, 2007, Effect of ultrasound on HDPE/clay nanocomposites: rheology, structure and properties, *Polymer* **48**, 281-289.

Ye, Y. S., H. B. Kim, N. S. Kim and J. W. Lee, 2005, A study on analysis of polymer extruder process using finite element method, *The Korean Society of Mech. Eng.* Part A **29**, 1, 145-155.

Youn, B. D. and K. K. Choi, 2004, A new response surface methodology for reliability based design optimization, *Computers and Structures* **82**, 241-256.